



Pyrazolopyrimidines as dual Akt/p70S6K inhibitors

Kenneth D. Rice, Moon H. Kim^{*,†}, Joerg Bussenius^{*}, Neel K. Anand, Charles M. Blazey, Owen J. Bowles, Lynne Canne-Bannen, Diva S.-M. Chan, Baili Chen, Erick W. Co, Simona Costanzo, Steven C. DeFina, Larisa Dubenko, Stefan Engst, Maurizio Franzini, Ping Huang, Vasu Jammalamadaka, Richard G. Khoury, Rhett R. Klein, A. Douglas Laird, Donna T. Le, Morrison B. Mac, David J. Matthews, David Markby, Nicole Miller, John M. Nuss, Jason J. Parks, Tsze H. Tsang, Amy L. Tshako, Yong Wang, Wei Xu

Exelixis, 210 E. Grand Avenue, South San Francisco, CA 94080, USA

ARTICLE INFO

Article history:

Received 9 February 2012

Revised 29 February 2012

Accepted 2 March 2012

Available online 10 March 2012

Keywords:

p70S6K inhibitor
Akt inhibitor
Pyrazolopyrimidine
PI3K pathway
Cancer

ABSTRACT

Activation of the PI3K/Akt/mTOR kinase pathway is frequently associated with human cancer. Selective inhibition of p70S6Kinase, which is the last kinase in the PI3K pathway, is not sufficient for strong tumor growth inhibition and can lead to activation of upstream proteins including Akt through relief of a negative feedback loop. Targeting multiple sites in the PI3K pathway might be beneficial for optimal activity. In this manuscript we report the design of dual Akt/p70S6K inhibitors and the evaluation of the lead compound **11b** in vivo, which was eventually advanced into clinical development.

© 2012 Elsevier Ltd. All rights reserved.

Hyperactivated signaling due to dysregulation of the phosphoinositide 3-kinase (PI3K)/Akt/mammalian target of rapamycin (mTOR) pathway is observed in many cancers.¹ The potential for therapeutic intervention by inhibiting one or more targets in this pathway has been extensively discussed in the literature.^{2–6} Some of the first compounds to enter the clinic were analogs of rapamycin, which are all highly specific inhibitors of mTORC1.⁷ Although these compounds have shown great promise in preclinical models, and have demonstrated clinical activity in select indications, they have not shown broad spectrum clinical activity in single agent trials.⁸ This may be in part due to the presence of a negative feedback mechanism, whereby inhibition of mTORC1 induces insulin receptor substrate IRS-1 expression leading to upregulation of IGF1R-dependent signaling, which then leads to activation of PI3K and its downstream effectors, in particular Akt.⁹ The upregulation of S473 phosphorylated Akt was observed in vitro in different cancer cell lines as well as in vivo in human tumors.⁹

In a recent disclosure we have described the SAR and synthesis of pyrazolopyrimidines as potent and selective p70S6K inhibitors

resulting in lead compound **1a** (Table 1).¹⁰ While **1a** represented a substantial improvement over the initial HTS hit and demonstrated tumor growth inhibition in vivo, it also showed a similar upregulation of pAkt(S473) in pharmacodynamic studies. This effect can likely be explained by induction of the same negative feedback loop, which would then account for the relative weak activity in the efficacy experiment considering the high potency of compound **1a**. These observations encouraged us to determine if we could compensate for the upregulated Akt activity by reducing the selectivity of compound **1a** and adding Akt inhibitory properties into the molecule.

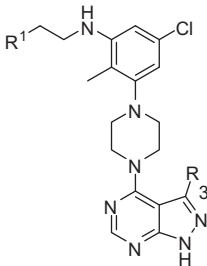
The SAR leading to **1a** has shown that replacing the 3-position ethyl group on the pyrazolopyrimidine with a bromine resulted in less selectivity and higher enzymatic Akt activity (see compounds **2a,b** Table 1).¹¹ We then determined the cellular potency of these compounds in two different cell lines, A549 and PC-3, which also served as in vivo models. The assays measured the inhibition of phosphorylation of ribosomal protein S6 to quantify p70S6K activity, and of GSK3 β , a known Akt substrate, for quantifying Akt activity.^{12,13} The higher biochemical Akt activity of the bromo analogs compared to the ethyl compounds had no effect on S6 phosphorylation in A549 cells, but did result in higher potency in the PC-3 cell line. The higher enzymatic Akt activity of the bromo analogs also led to increased cellular Akt potency over the ethyl compounds in PC-3 cells, as measured by inhibition of phosphorylation of GSK3 β , especially when R¹ was a pyrrolidine.

* Corresponding authors. Tel.: +82 31 920 2773; fax: +82 31 920 1571 (M.H.K.); tel.: +1 650 837 7000; fax: +1 650 837 8177 (J.B.).

E-mail addresses: mkim58@ncc.re.kr (M.H. Kim), jbussenius@exelixis.com (J. Bussenius).

[†] Present address: National Cancer Center, 323 Ilsan-ro, Ilsandong-gu, Goyang-si, Gyeonggi-do 410-769, Republic of Korea.

Table 1
Activities for compounds **1a,b** and **2a,b**



ID	R	R ¹	p70S6K IC ₅₀ (nM)	Akt1 IC ₅₀ (nM)	Cell S6-p IC ₅₀ (nM)A549/PC-3	Cell GSK3β-p IC ₅₀ (nM)PC-3	Mouse liver microsome stability (% conversion) ^a
1a	Et	NMe ₂	2	371	45/211	9026	29
1b	Et		3	434	80/832	3589	18
2a	Br	NMe ₂	2	53	43/141	4285	50
2b	Br		2	42	94/446	1271	19

^a After 30 min incubation at 15 μM compound concentration and 0.5 mg/mL microsome concentration.

As expected, the pyrrolidines **1b** and **2b** also have the additional advantage of higher metabolic stability compared to the dimethylamine analogs **1a** and **2a** expressed by their mouse liver microsomal degradation. On the basis of these in vitro data we decided to use compound **2b** as starting point for further SAR optimization with the help of computer modeling.

We began our study by docking the literature Akt inhibitor **3** (Fig. 1)¹⁴ into the crystal structure of active Akt (PDB code 1O6L) and compared the results with the docking of our early p70S6K inhibitor **4** in the same structure. The superimposition of the two compounds showed some overlap, particularly in the proposed binding site on the kinase hinge region, but also revealed that the hydrophobic pocket containing the benzophenone moiety of compound **3** was unoccupied by our scaffold (Fig. 2). Extension with a hydrophobic group off the 5'-position, where the chlorine substituent is located, should allow access to this pocket. This motivated us to focus our lead optimization efforts on increasing the interactions with this pocket and therefore the Akt kinase potency.

In order to test our model a number of analogs with different structural motifs at the 5'-position were synthesized and are shown in Table 2 (compounds **5–11**).

The synthesis of compounds **1a,b**, **2a**, and **4** was described in our recent disclosure and compound **2b** was prepared in a analogous manner.¹⁰ Compounds **5a,b** and **8** in Table 2 were made as shown in Scheme 1. Alkylation of phenol **12** with either ethyl or isobutyl bromide gave the ethers **13a,b**. Successive Buchwald–

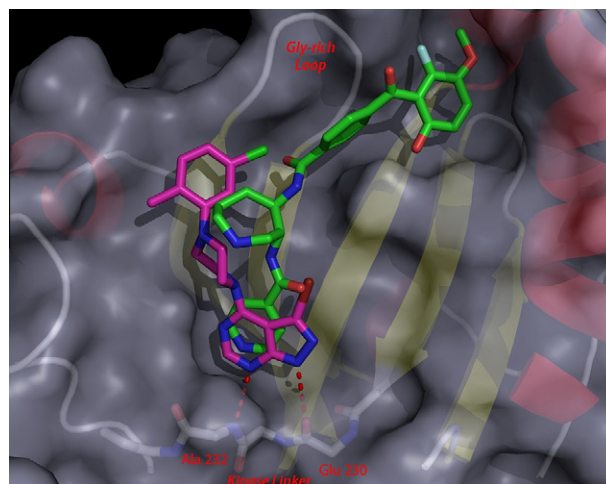


Figure 2. Docking of Akt inhibitor **3** and p70S6K inhibitor **4** into the crystal structure of Akt.

Hartwig amination with Boc-piperazine followed by 2-pyrrolidine-1-yl-ethylamine afforded compounds **15a,b**, which were deprotected and reacted with 3-bromo-4-chloro-1*H*-pyrazolo[3,4-*d*]pyrimidine to give the desired products **5a,b**. Successive amination of phenol **12** as above followed by activation as triflate and Sonogashira reaction with *tert*-butylacetylene afforded intermediate **17**, which was converted to the alkylphenyl derivative **18** by hydrogenolysis. Finally, conversion to compound **8** was achieved as described above.

The preparation of the remaining compounds **6**, **7**, **9**, **10** and **11a,b** in Table 2 is illustrated in Scheme 2. Central starting material for all compounds was methyl ester **19**. Successive Buchwald–Hartwig amination of **19** with Boc-piperazine and 2-pyrrolidine-1-yl-ethylamine, followed by deprotection and reaction with 3-bromo-4-chloro-1*H*-pyrazolo[3,4-*d*]pyrimidine gave ester **10**. Saponification of **19** followed by conversion to the methyl oxadiazole **23** and then repetition of the above described steps yielded compound **9**. Buchwald–Hartwig amination of **19** to intermediate **20**, followed by ester hydrolysis and amide coupling with aniline afforded amide **24**. A second amination, then deprotection and final coupling to the pyrimidine gave compound **6**. In a similar manner, successive aminations of **19**, saponification and amide coupling

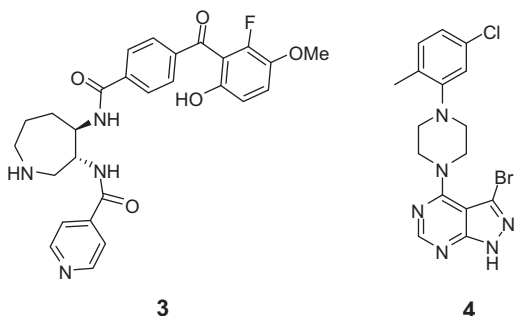
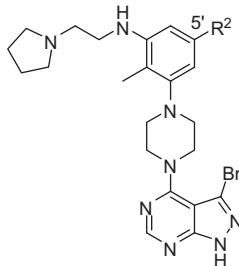
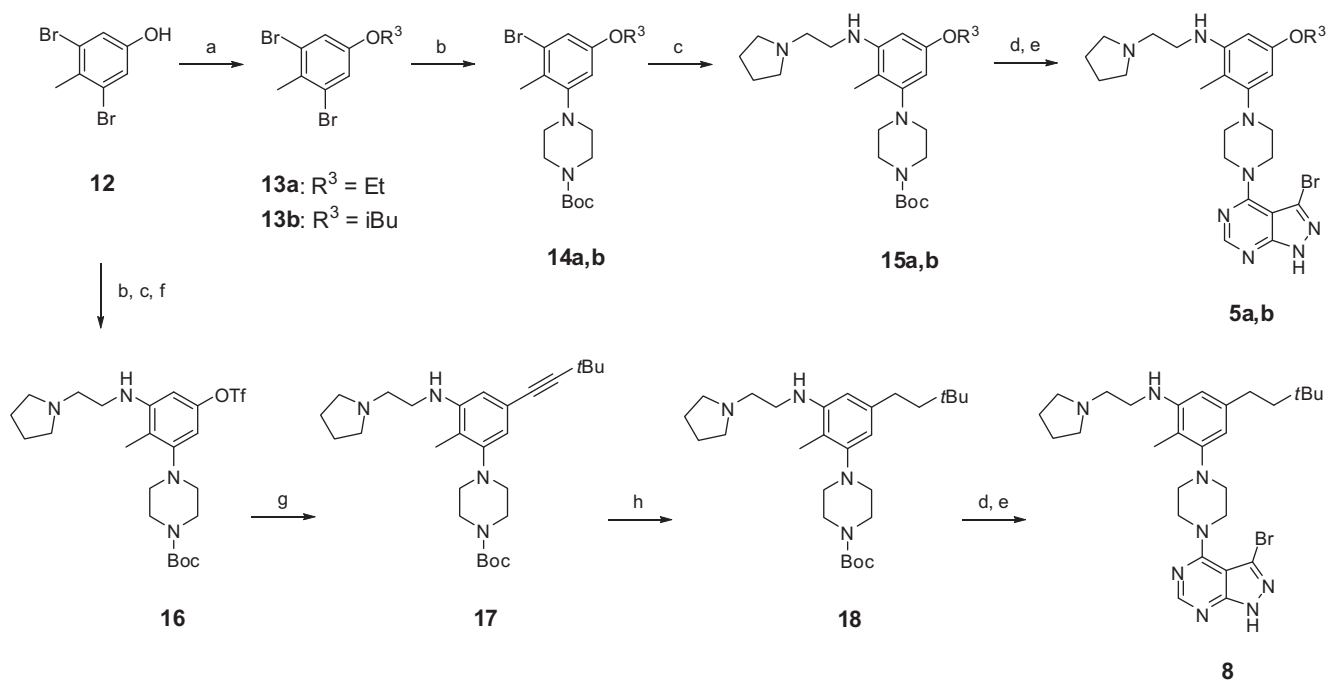


Figure 1. Structures of Roche Akt inhibitor **3** and compound **4**.

Table 2
Biochemical and cellular activities for analogs **2b** and **5–11**



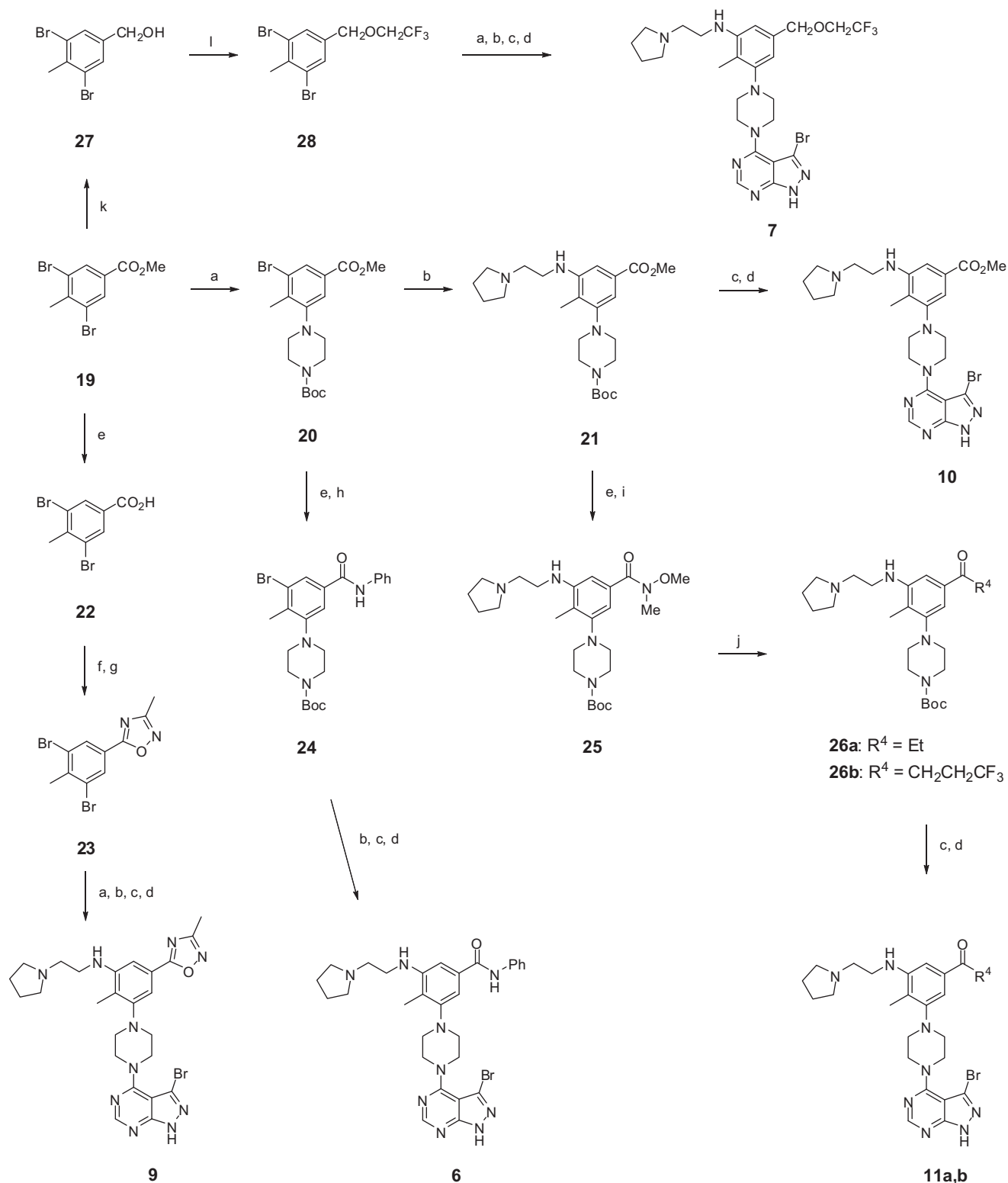
ID	R ²	p70S6K IC ₅₀ (nM)	Akt1 IC ₅₀ (nM)	Cell S6-p IC ₅₀ (nM) A549/PC-3	Cell GSK3β-p IC ₅₀ (nM) PC-3
2b	Cl	2	42	94/446	1507
5a	–OEt	2	56	197/–	9067
5b	–OiBu	1	9	37/214	700
6	–CONHPh	1	13	14/190	7811
7	–CH ₂ OCH ₂ CF ₃	2	8	17/66	730
8	–CH ₂ CH ₂ tBu	2	7	116/203	1982
9		1	6	13/47	665
10	–CO ₂ Me	2	5	44/52	1843
11a	–CO–CH ₂ CH ₃	1	5	18/25	976
11b	–CO–CH ₂ CH ₂ CF ₃	2	1	30/55	194



Scheme 1. Preparation of compounds **5a,b** and **8** in Table 2. Reagents and conditions: (a) R³Br, Cs₂CO₃, DMF, rt, 16 h; (b) Boc-piperazine, toluene, Pd₂(dba)₃, BINAP, NaOtBu, 110 °C, 16 h; (c) 2-pyrrolidine-1-yl-ethylamine, toluene, Pd₂(dba)₃, BINAP, NaOtBu, 110 °C, 16 h; (d) HCl, dioxane, MeOH, reflux, 2 min; (e) 3-bromo-4-chloro-1H-pyrazolo[3,4-d]pyrimidine, iPrOH, DIEA, 60 °C, 2 h; (f) triflic anhydride, CH₂Cl₂, triethylamine, –78 °C, 30 min, then rt, 16 h; (g) *tert*-butylacetylene, DMF, PdCl₂(PPh₃)₂, CuI, triethylamine, 100 °C, 16 h; (h) hydrogen, Pd/C, ethyl acetate, 2 h.

afforded Weinreb amide **25**, which was converted by Grignard reaction into the ketones **26a,b**. Completion of the sequence with the already described final two steps gave the ketones **11a,b**. Finally, reduction of ester **19** to the hydroxymethyl derivative **27** followed by Mitsunobu reaction with trifluoroethanol afforded ether **28**, which was converted by the remaining sequence to compound **7**.

Interestingly, none of the different substituents affected the biochemical p70S6K activity, but as the model predicted, larger hydrophobic groups in the 5'-position indeed increased the biochemical Akt activity. Particularly illustrative were two pairs of compounds, ethers **5a** and **5b**, and ketones **11a** and **11b**, where the increased size of the substituent resulted in an about five-fold improvement in biochemical Akt activity. For these examples the higher biochemical



Scheme 2. Preparation of compounds **6**, **7**, **9**, and **11a,b** in Table 2. Reagents and conditions: (a) Boc-piperazine, toluene, Pd₂(dba)₃, BINAP, NaOtBu, 110 °C, 16 h; (b) 2-pyrrolidine-1-yl-ethylamine, toluene, Pd₂(dba)₃, BINAP, NaOtBu, 110 °C, 16 h; (c) HCl, dioxane, MeOH, reflux, 2 min; (d) 3-bromo-4-chloro-1*H*-pyrazolo[3,4-*d*]pyrimidine, *i*PrOH, DIEA, 60 °C, 2 h; (e) KOH, methanol, water, 60 °C, 2 h; (f) *N*-hydroxyethanimidamide, DMF, HATU, DIEA, rt, 16 h; (g) TBAF, THF, rt, 15 h; (h) aniline, DMF, HATU, HOAt, *N*-methylmorpholine, rt, 17 h; (i) *N,O*-dimethylhydroxylamine, HATU, HOAt, *N*-methylmorpholine, rt, 17 h; (j) R⁴MgBr, THF, 0 °C, then rt, 16 h; (l) CF₃CH₂OH, benzene, 1,1'-(azodicarbonyldipiperidine), tri-*n*-butylphosphine, rt, 6 h.

activity translated into a similar improvement in cell based potency, as measured by inhibition of phosphorylation of GSK3 β . However, this correlation of biochemical and cellular activity was not always observed, although there was clearly a general trend.

For compounds with cellular IC₅₀s less than 1 μ M the pharmacokinetic profiles in the rat were evaluated (Table 3). Also the mouse plasma exposures at 100 mg/kg were determined, since this was the model for further pharmacodynamic and efficacy studies.

Table 3
Rat PK and mouse plasma exposure for compounds **5b**, **7**, **9**, and **11a,b**

ID	Species	Dose (mg/kg)	CL (mL/h/kg)	V _d (L/kg)	T _{1/2} (h) IV/PO	F (%)	C _{max} (μM) IV/PO	AUC/dose (μM h kg/mg) IV/PO	Mouse plasma exposure at 100 mg/kg, 1 and 4 h (μM)
5b	Rat	5	4769	14.7	2.5/1.7	13	1.15/0.07	0.35/0.05	1.2/1.3
7	Rat	2.5	3809	9.7	2.1/1.4	11	0.39/0.02	0.43/0.05	1.2/1.2
9	Rat	2.5	4382	14.2	2.4/2.9	10	0.37/0.01	0.45/0.05	0.3/0.1 ^a
11a	Rat	5	2940	10.5	3.1/2.9	28	1.44/0.14	0.56/0.15	2.0/2.0
11b	Rat	2.5	2722	12.9	3.5/7.9	35	0.33/0.04	0.64/0.17	1.6/3.1
11b	Dog	3	1562	17.0	7.5/10.4	58	0.21/0.10	0.95/0.54	
11b	Monkey	3	1230	6.9	6.1/6.4	77	0.58/0.40	1.22/0.94	

^a At 30 mg/kg.

Unfortunately, most compounds like the ether **5b**, the fluorinated ethyloxymethyl analog **7**, and the oxadiazole **9** showed low absorption and oral bioavailability. Only the ketones **11a** and **11b** had significantly improved values. The pharmacokinetic profile of the most active compound, ketone **11b** was then also obtained in the dog and monkey, where it showed even higher oral bioavailabilities of 58% and 77%, respectively.

On the basis of the high biochemical activity and cellular potency combined with good oral bioavailability in different species, we decided to advance compound **11b** into a pharmacodynamic study, in which the inhibition of S6-, GSK3β-, and PRAS40- (another downstream target of Akt) phosphorylation was measured. The compound was dosed at 100 mg/kg bid with a total of five doses before measurement in the PC-3 prostate carcinoma model and demonstrated 90% inhibition of S6-p, 46% inhibition of GSK3β-p, and 76% inhibition of PRAS40-p. Compound **11b** was subsequently evaluated in a PC-3 xenograft efficacy experiment and dosed orally at 50 mg/kg qd for 15 days. In this study **11b** resulted in 52% tumor growth inhibition (TGI), compared to 49% TGI for the selective p70S6K inhibitor **1a** at 100 mg/kg.¹⁰ The efficacy of compound **11b** was also determined in the A549 breast cancer model and dosed orally at 50 mg/kg qd and 100 mg/kg qd for two days every 4 days. The compound was highly active in this study with 71% tumor growth inhibition for the 50 mg/kg dose and 96% TGI for the 100 mg/kg alternate dosing schedule as a single agent.

In summary, we have described the successful optimization of a selective p70S6K inhibitor **1a** into a dual Akt/p70S6K inhibitor **11b**. The additional Akt activity is reflected in better efficacy in xenograft studies compared to **1a**. Due to its excellent activity in vitro and in vivo combined with good oral bioavailability in higher species, compound **11b** was nominated as clinical candidate and went into development as an oral agent for use in patients with solid tumors and hematological malignancies under the name XL418.

Acknowledgment

The authors thank Paul Foster for his graphical support.

References and notes

- Vivanco, I.; Sawyers, C. L. *Nat. Rev. Cancer* **2002**, *2*, 489.
- Yap, T. A.; Garrett, M. D.; Walton, M. I.; Raynaud, F.; DeBono, J. S.; Workman, P. *Curr. Opin. Pharmacol.* **2008**, *8*, 393.
- Hennessy, B. T.; Smith, D. L.; Ram, P. T.; Lu, Y.; Mills, G. B. *Nat. Rev. Drug Disc.* **2005**, *4*, 988.
- Engelman, J. A. *Nat. Rev. Cancer* **2009**, *9*, 550.
- Liu, P.; Cheng, H.; Roberts, T. M.; Zhao, J. J. *Nat. Rev. Drug Disc.* **2009**, *8*, 627.
- Courtney, K. D.; Corcoran, R. B.; Engelman, J. A. *J. Clin. Oncol.* **2010**, *28*, 1075.
- Serra, V.; Scaltriti, M.; Prudkin, L.; Eichhorn, P. J. A.; Ibrahim, Y. H.; Chandralapaty, S.; Markman, B.; Rodriguez, O.; Guzman, M.; Rodriguez, S.; Gili, M.; Russillo, M.; Parra, J. L.; Singh, S.; Arribas, J.; Rosen, N.; Baselga, J. *Oncogene* **2011**, *30*, 2547.
- Cloughesy, T. F.; Yoshimoto, K.; Nghiemphu, P.; Brown, K.; Dang, J.; Zhu, S.; Hsueh, T.; Chen, Y.; Wang, W.; Youngkin, D.; Liau, L.; Martin, N.; Becker, D.; Bergsneider, M.; Lai, A.; Green, R.; Ogleby, T.; Koleto, M.; Trent, J.; Horvath, S.; Mischel, P. S.; Mellinghoff, I. K.; Sawyers, C. L. *PLoS Med.* **2008**, *5*, 139.
- O'Reilly, K. E.; Rojo, F.; She, Q.-B.; Solit, D.; Mills, G. B.; Smith, D.; Lane, H.; Hofmann, F.; Hicklin, D. J.; Ludwig, D. L.; Baselga, J.; Rosen, N. *Cancer Res.* **2006**, *66*, 1500.
- Bussenius, J.; Anand, N. K.; Blazey, C. M.; Bowles, O. J.; Canne Bannen, L.; Chan, D. S. M.; Chen, B.; Co, E. W.; Costanzo, S.; DeFina, S. C.; Dubenko, L.; Engst, S.; Franzini, M.; Huang, P.; Jammalamadaka, V.; Khoury, R. G.; Kim, M. H.; Klein, R. R.; Laird, D.; Le, D. L.; Mac, M. B.; Matthews, D. J.; Markby, D.; Miller, N.; Nuss, J. M.; Parks, J. J.; Tsang, T. H.; Tshako, A. L.; Wang, Y.; Xu, W.; Rice, K. D. *Bioorg. Med. Chem. Lett.* **2012**, *12*, 2283.
- p70S6K and Akt1 assay: Kinase activity was measured as the percent of ATP consumed following the kinase reaction using luciferase–luciferin-coupled chemiluminescence. Reactions were conducted in 384-well white, medium binding microtiter plates (Greiner). Kinase reactions were initiated by combining test compounds, 500 nM ATP, and kinase in 20 μL of reaction buffer (20 mM Hepes pH 7.5, 10 mM MgCl₂, 0.03% NP40, 0.03% BSA, 1 mM DTT). The reaction mixture was incubated at ambient temperature for 3 h after which 20 μL aliquot of luciferase–luciferin mix (50 mM HEPES, pH 7.8, 67 mM oxalic acid (pH 7.8), 5 (or 50) mM DTT, 0.4% Triton X-100, 0.25 mg/mL coenzyme A, 63 mM AMP, 28 mg/mL luciferin and 40,000 units/mL luciferase) was added and the chemiluminescence signal measured using a Victor2 plate reader (Perkin–Elmer).
- pS6 assay in cells: A549 (ATCC, CCL-185) or PC-3 (ATCC, CRL-1435) cells were seeded in 96-well plates (NUNC) in DMEM (Cellgro) containing heat inactivated 10% FBS (Hyclone), 1% penicillin–streptomycin (Cellgro), and 1% non-essential amino acids (Cellgro) at 7.5×10^3 cells/well. Cells were incubated at 37 °C, 5% CO₂ for 48 h. Test compound in DMSO was diluted in DMEM. The DMSO concentration in cell culture medium was maintained at 0.2% in all wells. Cells were treated with diluted compound and each concentration assayed in triplicate at concentrations of 1.2–300 nM. 0.004–1 nM rapamycin (Cell Signaling Technology, 9904) and 0.12–30 nM staurosporine (Calbiochem, 569396) served as positive controls. Negative control wells were treated with DMSO. Cells were incubated for 3 h at 37 °C, 5% CO₂ for 3 h in the presence of compound. Post compound treatment cells were fixed as follows: medium was removed and 100 μL/well of 4% formaldehyde (Sigma–Aldrich, 08920AD) in TBS (Pierce, 28376) was added to each well at room temperature (RT) for 20 min. Cells were quenched with 100 μL 0.6% H₂O₂ (VWR International, 43038308) in TBS (Pierce, 28376) + 0.1% Tween20 (Sigma, P-7949) (TBST) for 20 min at rt. Plates were washed 3 × with 200 μL TBS and blocked with 100 μL 5% BSA (Jackson ImmunoResearch Laboratory, 001-000-162 unless otherwise noted) in TBST for 1 h at rt. Anti-phospho-S6 ribosomal protein antibody (Cell Signaling Technology, Ser 240/244 2212L) and anti-total-S6 ribosomal protein antibody (Cell Signaling Technology, 2215L) were diluted 1:200 in 5% BSA (Jackson ImmunoResearch Laboratory, 64004) in TBST. Fifty microliter primary antibody solution was added to each well and incubated overnight at 4 °C. Plates were washed 3 × with 200 μL TBST. Goat anti-rabbit secondary antibody (Chemicon International, 24070101) was diluted at 1:20000 in 5% non-fat dry milk in TBST. Fifty microliter of antibody solution was added to each well and incubated for 1 h at rt. Plates were washed 3 × with 200 μL TBST and 2 × 200 μL TBS. Chemiluminescent substrate (Super Signal Elisa Femto Chemiluminescent Substrate; Pierce, 37075) was prepared at rt. Hundred microliter of chemiluminescent substrate per well was added and then the plate was shaken for 1 min. Luminescence was read immediately on a Wallac plate reader.
- GSK3β cell assay in PC-3 cells: PC-3 cells were seeded in 96-well plates in DMEM containing heat-inactivated 10% FBS, 1% penicillin–streptomycin, and 1% non-essential amino acids at 7.5×10^3 cells/well. Cells were incubated at 37 °C, 5% CO₂ for 24 h and then starved in serum-free medium for 24 h. Test compound in DMSO was diluted in DMEM. The DMSO concentration in cell culture medium was maintained at 0.2% in all wells. Cells were treated with diluted compound and each concentration assayed in triplicate at concentrations of 12–3000 nM. 1.2–300 nM staurosporine served as a positive control. Negative control wells were treated with DMSO. Cells were incubated for 3 h at 37 °C, 5% CO₂ in the presence of compound followed by stimulation with 100 ng/mL IGF1 (Upstate Biotechnology, 01-189) for 30 min. Post compound treatment cell plates were processed as described for the pS6 cell assay except that the primary antibodies were Anti-phospho-GSK3β(S9) (Cell Signaling Technology, 9336) and anti-total-GSK3β (Cell Signaling Technology, 9332) diluted 1:200 in 5% BSA in TBST.
- Breitenlechner, C. B.; Wegge, T.; Berillon, L.; Graul, K.; Marzenell, K.; Friebe, W.-G.; Thomas, U.; Schumacher, R.; Huber, R.; Engh, R. A.; Masjost, B. *J. Med. Chem.* **2004**, *47*, 1375.